https://doi.org/10.5194/gmd-2020-179
Preprint. Discussion started: 7 July 2020

Geoscientific Model Development Discussions

Enhancement and validation of the state-of-the-art global hydrological model H08 (v.bio1) to simulate second-generation herbaceous bioenergy crop yield

Zhipin Ai[1], Naota Hanasaki[1], Vera Heck[2], Tomoko Hasegawa[3], Shinichiro Fujimori[4]

[1]Center for Climate Change Adaptation, National Institute for Environmental Studies, 16-2, Onogawa, Tsukuba 305-8506, Japan

[2]Potsdam Institute for Climate Impact Research, Telegraphenberg A 31, Potsdam 14473, Germany

[3]Department of Civil and Environmental Engineering, Ritsumeikan University, 56-1, Toji-in Kitamachi, Kita-ku, Kyoto 603-8577, Japan

[4]Department of Environmental Engineering, Kyoto University, Building C1-3, C-cluster, Kyoto-Daigaku-Katsura, Nishikyo-ku, Kyoto 615-8504, Japan

Correspondence to: Zhipin Ai (ai.zhipin@nies.go.jp)

Abstract. Large-scale deployment of bioenergy plantations would have adverse effects on water resources. There is an increasing need to ensure the appropriate inclusion of the bioenergy crops in global hydrological models. Here, through parameter calibration and algorithm improvement, we enhanced the global hydrological model H08 to simulate the bioenergy yield from two dedicated herbaceous bioenergy crops, *Miscanthus* and switchgrass. Site-specific evaluations showed that the enhanced model had the ability to simulate yield for both *Miscanthus* and switchgrass, with the calibrated yields being well within the ranges of the observed yield. Independent country-specific evaluations further confirmed the performance of the enhanced H08. Using this improved model, we found that unconstrained irrigation more than doubled the yield of the rainfed condition, but reduced the water use efficiency (WUE) by 32% globally. With irrigation, the yield in dry climate zones can exceed the rainfed yields in tropical climate zones. Nevertheless, due to the low water consumption in tropical areas, the highest WUE was found in tropical climate zones, regardless of whether the crop was irrigated. Our enhanced model provides a new tool for the future assessment of bioenergy–water tradeoffs.

https://doi.org/10.5194/gmd-2020-179
Preprint. Discussion started: 7 July 2020

Geoscientific Model Development Discussions

1 Introduction

The bioenergy with carbon capture and storage (BECCS) technology enables the production of energy without carbon emissions, while sequestering carbon dioxide from the atmosphere, producing negative emissions. Therefore, BECCS is considered an important technology in the push to achieve the 2-degree climate target (Smith et al., 2015). With ambitious climate policies, the demand for bioenergy in 2100 could reach 200–400 EJ per year, based on recent predictions (Rose et al., 2013; Bauer et al., 2018). However, large-scale deployment of BECCS requires that water consumption be doubled or even tripled, which would exacerbate the future water scarcity (Beringer et al., 2011; Bonsch et al., 2016; Hejazi et al., 2015; Yamagata et al., 2018). Therefore, representation of bioenergy crops in global hydrological models is critical to better investigate the possible side effects of large-scale implementation of BECCS.

Second-generation bioenergy crops, such as *Miscanthus* and switchgrass, are generally regarded as a dedicated bioenergy source due to the high yield potential and their lack of direct competition with food production (Beringer et al., 2011; Yamagata et al., 2018; Wu et al., 2019). This is because *Miscanthus* and switchgrass are rhizomatous perennial C4 grasses, which have a high photosynthesis efficiency (Trybula et al., 2015). These two crops have been included in a series of models including Lund–Potsdam–Jena managed Land (LPLml) (Beringer et al., 2011; Bondeau et al., 2007), ORCHIDEE (Li et al., 2018), the High-Performance Computing Environmental Policy Integrated Climate model (HPC-EPIC) (Kang et al., 2014; Nichols et al., 2011), the Community Land Model (version 5) (CLM5) (Cheng et al., 2020), MISCANMOD (Clifton-Brown et al., 2000; 2004), MISCANFOR (Hastings et al., 2009), Agricultural Production Systems Simulator (APSIM) (Ojeda et al., 2017), and the Soil & Water Assessment Tool (SWAT) (Trybula et al., 2015). However, among these models, only LPLml includes the global implementation of the schemes for irrigation, water withdrawal, and river routing. This severely limits the application of the models to address the global bioenergy–water tradeoffs or synergies.

To the best of our knowledge, LPJml is the first global model that includes both biogeny and the water cycle. It has therefore been widely used to quantify the water effects of the large-scale deployment of BECCS in many earlier studies (Beringer et al., 2011; Heck et al., 2016; 2018; Bonsch et al., 2016; Janes et al., 2018; Stenzel et al., 2019). However, it should be noted that *Miscanthus* and switchgrass are not distinguished in LPLml, which instead uses a C4 grass to parameterize them. A separate parametrization for the two bioenergy crops could enhance the BECCS simulation since they showed totally different plant characteristics and crop yield (Heaton et al., 2008; Trybula et al., 2015; Li et al., 2018). H08 is a global hydrological model that considers human activities, including reservoir operation, aqueduct water transfer, seawater desalination, and water abstraction for irrigation, industry, and municipal use (Hanasaki et al., 2008a, 2008b, 2010, 2018a, 2018b). The first use of H08 to simulate the bioenergy crop yield was reported in an impact assessment of the effects of BECCS on water, land, and ecosystem services (Yamagata et al., 2018). Another recent study also used H08 estimates of yield for *Miscanthus* and switchgrass to predict global advanced bioenergy potential (Wu et al., 2019). The first bioenergy crop implementation in H08 was conducted by two steps. First, crop parameters for *Miscanthus* and switchgrass were adopted based on the settings from the SWAT model 2012 version (Arnold et al., 2013). Second, because both *Miscanthus* and switchgrass are perennial, the potential heat unit was set as unlimited. Maturity was defined by either undergoing an autumn freeze (i.e., the air temperature was below the minimum temperature for growth) or the exceedance of the maximum of 300 continuous days of growth. However, it is noted that the model performance for the simulated bioenergy crop yield was not validated at all.

The objective of this study was to enhance and validate the ability of H08 to simulate the second-generation herbaceous bioenergy crop yield. The following sections of this paper will: 1) describe the default biophysical process of the crop module in H08, 2) explain the enhancement of H08 for *Miscanthus* and switchgrass, 3) evaluate the enhanced performance

https://doi.org/10.5194/gmd-2020-179
Preprint. Discussion started: 7 July 2020

of the model in simulating yields for *Miscanthus* and switchgrass, and 4) illustrate the effect of irrigation on the yield, water consumption, and WUE of *Miscanthus* and switchgrass.

2 Materials and methods

2.1 H08 and its crop module

H08 is a global hydrological model (Hanasaki et al., 2008a, 2008b). H08 can simulate the basic natural and anthropogenic hydrological process as well as crop growth at a spatial resolution of 0.5° and at a daily interval. The six sub-modules are coupled in a unique way. The land surface module can simulate the main water cycle components, such as evapotranspiration and runoff. The former is used in the crop module, and the latter is used in the river routing and environmental flow modules. The agricultural water demand simulated by the crop module and the streamflow simulated by the river routing and reservoir operation module finally enter into the withdrawal module. A graphical diagram illustrating these coupled relationships can be found in Hanasaki et al. (2008b).

Figure 1 shows the basic biophysical process of the crop module in H08. The biomass accumulation is based on Monteith et al. (1977). The crop phenology development is based on daily heat unit accumulation theory. The harvest index is used to partition the grain yield. Regulating factors, including water and air temperature, are used to constrain the yield variation (see supplementary material for information on the algorithms). The crop module can simulate the potential yield, crop calendar, and irrigation water consumption for 18 crops, including barley, cassava, cotton, peanut, maize, millet, oil palm, potato, pulses, rape, rice, rye, sorghum, soybean, sugar beet, sugarcane, sunflower, and wheat. The parameters for these crops were taken from those of the SWAT model. To better reflect the agronomy practice, H08 divides each simulation cell into four sub-cells: rainfed, single-irrigated, double-irrigated, and other (i.e., non-agricultural land uses).

2.2 Enhancement of H08 for *Miscanthus* and switchgrass

To establish its ability to address perennial bioenergy crops, the crop sub-module of H08 was enhanced to include functions for the second-generation bioenergy crops *Miscanthus giganteus* and the switchgrass *Panicum virgatum* as follows. First, we changed the leaf area development curve by adopting the potential heat unit (Hun) and leaf area related parameters (dpl1 and dpl2) proposed by Trybula et al. (2015). The potential heat unit can determine both the total cropping days and the leaf development. Here, we set it at 1,830 and 1,400 degrees for *Miscanthus* and switchgrass, respectively, as recommended by Trybula et al. (2015) based on their field observations. The dpl1 and dpl2 parameters (see Table 1), which were used for determining the leaf development curve, were also changed to the values suggested by Trybula et al. (2015). This modification substantially changed the original heat unit index (Ihun) and the development of the leaf area index curve. Second, we modified the algorithm for water stress that was used to regulate the radiation use efficiency. We took the ratio of actual evapotranspiration to potential evapotranspiration as the water stress factor for any point in the simulation, similar to the description of the soil moisture deficit used in other studies (Anderson et al., 2007; Yao et al., 2010). Third, we conducted parameter calibrations based on a series of simulations. The calibration process is presented in section 2.5, and the finalized parameter settings are given in Table 1 and section 3.1. Fourth, we added as an output item the water consumption of *Miscanthus* and switchgrass to analyze the water consumption and WUE in the crop sub-module. Fifth, we fixed the bug in the original code. For definitions and the functions of the above parameters, such as Hun, dpl1, dpl2, and Ihun, please see the algorithm descriptions in the supplementary material.

2.3 Model input data

The WATCH-Forcing-Data-ERA-Interim (WFDEI) global meteorological data (Weedon et al., 2014) from 1979 to 2016 were used in all simulations. The WFDEI data were based on the methodology used for WATer and global CHange

https://doi.org/10.5194/gmd-2020-179
Preprint. Discussion started: 7 July 2020

(WATCH) forcing data by utilizing ERA-Interim global reanalysis data. The data cover the whole globe at a spatial resolution of 0.5°. Eight daily meteorological variables (air temperature, wind speed, air pressure, specific humidity, rainfall, snowfall, and downward shortwave and longwave radiation) were used to run H08.

2.4 Yield data

To independently calibrate and validate the performance of H08 in simulating the bioenergy yield, we collected and compiled up-to-date site-specific and country-specific yield data from both observations and simulations (Clifton-Brown et al., 2004; Searle and Malins, 2014; Heck et al., 2016; Kang et al., 2014; Li et al., 2018a). A map showing the locations of the majority of sites under the rainfed condition is presented in Fig. 2. The data sites were predominantly distributed in Europe and the US. It should be noted that the sites are generally located in temperate and continental climate zones, with few located in the tropics and dry climate zones. Detailed lists of the sites from which the yields of *Miscanthus* and switchgrass were reported are documented in Tables S1 and S2 (for the rainfed condition) and Table S3 (for the irrigated condition) in the supplementary material.

2.5 Simulation and analysis

Simulations were conducted at the daily scale with annual meteorological conditions within the period 1979–2016 (38 years). Two simulations were run with different purposes. The first simulation was conducted with the land surface module and the crop module without irrigation to calibrate and validate both the original and enhanced H08 models. The second simulation was also conducted with the land surface module and the crop module but with irrigation to investigate the yield potential under irrigated conditions with the enhanced H08. It should be noted that irrigation in this study means uniform unconstrained irrigation.

We conducted a calibration with the most sensitive parameters, such as radiation use efficiency (be), maximum leaf area index (blai), base temperature (Tb), maximum daily accumulation of temperature (Hunmax), and minimum temperature for planting (TSAW). The specific parameter ranges and steps set in the calibration process are shown in Table 2. In total, 1,944 simulations were conducted for *Miscanthus* and switchgrass to test all combinations of the parameter sets. The best parameter sets were selected using two steps: first, the lowest root mean square error (RMSE), and second, the highest correlation coefficient (R) of the simulated and observed yields within the lowest RMSE domain. Additional information on how these parameters affect the model can be found in the algorithm description section in the supplementary material. To conduct the calibration and validation, the observed site-specific data were used to calibrate the model, and the simulated country-specific data were used to validate the model. The site-specific data covered different latitudes, with ranges from 7.0°S to 56.8°N for *Miscanthus* and 28.45°N to 51.8°N for switchgrass. The collected country-specific data cover the three different models: MISCANMOD, HPC-EPIC, and LPJmL. This analysis provided an opportunity to illustrate yield-latitude relationships as well as the limitations and performance of the model. In addition, we introduced the Köppen climate classification into the source code to provide possible climate-specific analyses.

3 Results and discussion

3.1 Parameter calibration

Based on the optimal RMSE (4.68 and 3.16 Mg ha^{-1} yr^{-1} for *Miscanthus* and switchgrass, respectively) and R (0.67 and 0.53 for *Miscanthus* and switchgrass, respectively), we finalized the parameter set as shown in Table 1. The simulations presented in the table are for rainfed conditions because the few sites that were irrigated. The radiation-use efficiency was set at 38 and 22 (g MJ^{-1} × 10) for *Miscanthus* and switchgrass, respectively. These values are similar to those of previous reports. For example, values of 41 (g MJ^{-1} × 10) for Miscanthus and 17 (g MJ^{-1} × 10) for switchgrass were recommended by Trybula et al.

https://doi.org/10.5194/gmd-2020-179
Preprint. Discussion started: 7 July 2020

(2015). The base temperature was calibrated to be 8 and 10°C for *Miscanthus* and switchgrass, respectively. The base temperature is sensitive to the crop growing days. Ranges from 7 to 10°C for *Miscanthus* and from 8 to 12°C for upland switchgrass were suggested by Trybula et al. (2015). The calibrated values are within the above ranges. The maximum leaf area indices were calibrated at 11 and 8 for *Miscanthus* and switchgrass, respectively; these values were identical to those suggested by Trybula et al. (2015).

3.2 Site-specific performance of enhanced H08

An overview of the performance of the enhanced H08 is provided in Fig. 3. It can be seen that the performance of the enhanced H08 was improved over that of the original H08, with the tendency of overestimation for switchgrass and underestimation for *Miscanthus* having been successfully fixed. Points in a scatter plot comparing the simulated yield from the enhanced H08 with the observed yield were well distributed along the 1:1 line. More detailed site-specific results are shown in Figs. 4a (*Miscanthus*) and Fig. 4b (switchgrass). To depict the uncertainties in the observed yield, the minimum and maximum observed yields were added as error bars in Fig. 4. It was found that the simulated yields were within or close to the range of the observed yield. The simulated relative error was randomly distributed, substantially smaller than the range of the observed yield, and showed no climatic bias. This implies that the combination of the Hun identified by Tryubla et al (2015) and the calibrated parameters of this study are valid for climate zones other than that of the midwestern US, where the Hun was observed. Investigating the performance under the irrigated condition (shown in Fig. S1), we found that H08 performed well at sites 1, 2, and 10, but was out of range at the other sites. This could be attributed to the assumptions of irrigation. H08 assumes that irrigation is fully applied to crops. Therefore, if the reported yield is within the range of that between rainfed and irrigated crops, it is considered reasonable. This was found to be the case, as shown in Fig. S1. To investigate the uncertainty in the meteorological data, a simulation using other meteorological data from the S14FD dataset (Iizumi et al. 2017) was conducted; the results are compared in Fig. S2. The comparison showed that the WFDEI driven result was very similar to that obtained with the S14FD data.

3.3 Country-specific performance of enhanced H08

Figure 5 compares the yield simulated by the enhanced H08 with the collected independent country-specific yields simulated by MISCANMOD (Clifton-Brown et al., 2004), HPC-EPIC (Kang et al., 2014), and LPJmL (Heck et al., 2016). Here, the yield was simulated under rainfed conditions. For *Miscanthus*, the correlation coefficient of the yield simulated by H08 and MISCANMOD in the scatter plot (Fig. 5d) was 0.40. A t-test showed that the correlation was not significant at the 0.01 level. For consistency with the yield collected by MISCANMOD, any area within a country where the yield is less than 10 Mg ha^{-1} yr^{-1} was excluded from the analyses. Also, the land available for calculation was set as 10% of the pastureland and cropland. For switchgrass, the correlation coefficient of the yield simulated by H08 and HPC-EPIC in the scatter plot (Fig. 5e) was 0.80. A t-test showed that the correlation was significant at the 0.01 level. This indicates that the spatial pattern of the yield simulated by H08 was similar to that of HPC-EPIC. For example, high yields were found in Brazil, Colombia, Mozambique, and Madagascar, while low yields were found in Australia and Mongolia by both models.

Miscanthus and switchgrass are not distinguished in LPJmL, and we therefore compared the mixed (mean, *Miscanthus* and switchgrass) yield of *Miscanthus* and switchgrass simulated by H08 and the C_4 grass yield simulated by LPJmL. The correlation coefficient of the yield simulated by H08 and LPJmL in the scatter plot (Fig. 5f) was 0.78. A t-test showed that the correlation was significant at the 0.01 level. An additional comparison under the irrigated condition is presented in Fig. S3. The correlation coefficient of the yield simulated by H08 and LPJmL, as shown in the scatter plot (Fig. S3), was 0.95. A t-test showed that the correlation was significant at the 0.01 level. The difference was mainly due to Colombia, Sudan, Mozambique, and Mexico, which are located in tropical zones. The difference in these countries was generally equal to the

https://doi.org/10.5194/gmd-2020-179
Preprint. Discussion started: 7 July 2020

range of H08. For example, as shown in Fig. 5c, the yield in Colombia simulated by LPJmL was equal to the *Miscanthus* yield simulated by H08 (upper error bar). A separate comparison of the ensemble yield simulated by LPJmL, and the yield of *Miscanthus* and switchgrass simulated by H08 under both rainfed and irrigated conditions, is presented in Fig. S4. It can be seen that the yield of Miscanthus simulated by H08 was closer to the yield simulated by LPJml, which indicated that the LPJml-simulated yield was more likely to represent *Miscanthus*. This can also be inferred from the validation results in Heck et al. (2016).It was difficult to determine which model performed better due to the lack of observed data in tropical zones. This also indirectly indicated the relatively large uncertainty of the existing simulations in tropical zones (Kang et al., 2014).

The differences in model structure, use of specific algorithms, and the input climate data (different periods and sources) can induce differences in the yield simulated by MISCANMOD, HPC-EPIC, LPJmL, and H08. With regard to model structure, MISCANMOD uses a Kriging interpolation method to derive the spatial yield from the original site yield, whereas H08, LPJmL, and HPC-EPIC use grid-based calculations. H08 considers the single harvest system in tropical areas, whereas LPJml considers a multiple harvest system. With regard to the specific algorithms used, the water stress used to regulate radiation-use efficiency varies considerably among the models. The periods of climate data used as an input are 1960–1990, 1980–2010, and 1982–2005 for MISCANMOD, HPC-EPIC, and LPJmL, respectively. Here, the comparison was conducted with exactly the same period of HPC-EPIC and LPJmL. However, for MISCANMOD, we used the data from 1979–1990 in consideration of data availability. Note that the different meteorological data sources and spatial-temporal resolution would also contribute to these differences.

3.4 Spatial distribution of the simulated yield under rainfed and irrigated conditions

Figure 6 shows the global yield distribution of *Miscanthus* and switchgrass. Under rainfed conditions, high yields are distributed in eastern US, Brazil, southern China, Africa, and Southeast Asia. To evaluate the response of yield to irrigation, we compared two simulations under rainfed and irrigated conditions. As shown in Figs. 6c and 6d, unconstrained irrigation greatly increased yields, especially for areas in arid regions such as the western US, southern Europe, northeastern China, India, southern Africa, the Middle East, and coastal Australia. At the global scale, the increases (excluding the area with a polar climate) were 20.7 (from 16.8 to 37.5) Mg ha^{-1} yr^{-1} and 7.9 (from 7.4 to 15.3) Mg ha^{-1} yr^{-1} for *Miscanthus* and switchgrass, respectively, indicating that irrigation more than doubles the yield under rainfed conditions. The spatial distribution of yield increased due to the irrigation simulated by H08 being very similar to that simulated by LPJmL (Beringer et al., 2011). At the continental scale (e.g., Europe), the yield increase was mainly located in southern Europe, consistent with the findings obtained using MISCANMOD (Clifton-Brown et al., 2004). The yield response to irrigation for switchgrass was weaker than that for *Miscanthus* (see Figs. 6b and 6d). This might be due to a smaller dependency on water for switchgrass compared with *Miscanthus* (Mclsaac et al., 2010). *Miscanthus* growth has been reported to have a high water requirement due to the high yield, large leaf area index, and long growing season (Mclsaac et al., 2010; Lewandowski et al. 2003). As a result, the *Miscanthus* yield is strongly influenced by water availability, and an annual rainfall of 762 mm yr^{-1} is thought to be suitable for growth (Heaton et al., 2019). However, the precipitation in most locations is below this level, especially in arid and semi-arid regions (see Fig. S5 in the supplementary material). Therefore, irrigation plays a critical role in ensuring the optimum bioenergy crop yield in arid and semi-arid regions, especially for *Miscanthus*.

3.5 Effects of irrigation on yield, water consumption, and WUE in different climate zones

Climate is one of the main physical constraints of crop growth and yield. Figure 7a shows the mean yield for *Miscanthus* and switchgrass in four different Köppen climate zones (see Fig. S6 in the supplementary material). For *Miscanthus*, a tropical climate (including the northern part of South America, central Africa, Southeast Asia, and southern India) produced the highest average yield of 33.0 Mg ha^{-1} yr^{-1}. A temperate climate (including the eastern US, Europe, southern China, and the

https://doi.org/10.5194/gmd-2020-179
Preprint. Discussion started: 7 July 2020

southern part of South America) produced the second highest average yield of 19.7 Mg ha^{-1} yr^{-1}. Dry and continental climate zones had similar average yields of 8.3 and 6.2 Mg ha^{-1} yr^{-1}, respectively. For switchgrass, a tropical climate had the highest yield, averaging 11.9 Mg ha^{-1} yr^{-1}. For the other three climate types, the average yields averaged 9.0, 4.7, and 4.0 Mg ha^{-1} yr^{-1} for the temperate, continental, and dry climate zones, respectively. As shown in Fig. 7a, irrigation greatly increased the yield, especially in dry climate zones, which had the largest yield increases of 44.2 and 15.7 Mg ha^{-1} yr^{-1} for *Miscanthus* and switchgrass, respectively. In contrast, irrigation had a relatively weak effect on yield in the tropical climate zone.

Figure 7b shows the water consumption for both *Miscanthus* and switchgrass. The annual mean water consumption for *Miscanthus* was around 613 mm yr^{-1} for the tropical climate zone (with a high yield of 33.0 Mg ha^{-1} yr^{-1}), whereas it was 155 mm yr^{-1} for a dry climate (with a low yield of 8.3 Mg ha^{-1} yr^{-1}) under rainfed conditions. Under irrigated conditions, the largest increases in water consumption were 1,618 and 1,054 mm yr^{-1} for *Miscanthus* and switchgrass in dry climate zones, respectively. With such a large amount of irrigation, the yield in a dry climate zone can exceed that in a tropical climate zone under rainfed conditions. This highlights the yield-water tradeoff effects.

Figure 7c shows the WUE, which is defined in this study as the ratio of yield to water consumption. The WUE of *Miscanthus* in a tropical climate was 53.8 kg DM ha^{-1} mm^{-1} H_2O, and 53.5, 48.2, and 47.0 kg DM ha^{-1} mm^{-1} H_2O in dry, temperate, and continental climate zones under rainfed conditions. The WUE values of switchgrass were 41.2, 37.9, 30.4, and 29.7 kg DM ha^{-1} mm^{-1} H_2O in continental, dry, tropical, and temperate climate zones under rainfed conditions, respectively. The WUE values for *Miscanthus* were higher than those for switchgrass, which is inconsistent with values in previous reports (VanLoocke et al., 2012). With irrigation, the WUE decreased for both *Miscanthus* and switchgrass in all climate zones. Globally, excluding the area with a polar climate, the decreases were 14.2 (from 50.6 to 36.4) kg DM ha^{-1} mm^{-1} H_2O and 12.2 (from 34.8 to 22.6) kg DM ha^{-1} mm^{-1} H_2O for *Miscanthus* and switchgrass, respectively, indicating a reduction in the mean WUE values for *Miscanthus* and switchgrass of up to 32%. This is consistent with the current global WUE trend for crops, which is high for rainfed croplands but low for irrigated croplands. However, the general magnitude of this relationship changes if the site or regional scale is considered based on reports for wheat in Syria (Oweis et al., 2000) or for wheat and maize in the North China Plain (Mo et al., 2005). Note that it might be better to use a specific crop model to investigate water use efficiency at the site or watershed scale.

3.6 Improvements, uncertainties and limitations

Compared with earlier studies, our study made several important improvements. First, rather than using an approximation for C4 grass to represent *Miscanthus* and switchgrass in the LPJmL model, our enhanced H08 model simultaneously simulated the yields for *Miscanthus* and switchgrass at the global scale. Second, the hydrological effects of bioenergy crop production implemented in our model are actually not incorporated in some other models; for example, we considered irrigation and analyzed water use efficiency, which was not implemented in ORCHIDEE-MICT-BIOENERGY (Li et al 2018) and HPC-EPIC (Kang et al., 2014). Third, we investigated the differences in yield, water consumption, and WUE for both *Miscanthus* and switchgrass among different climate zones, which was useful for optimizing bioenergy land with better consideration of water protection. In summary, our enhanced model is the only global hydrological model that can simultaneously simulate *Miscanthus* and switchgrass with consideration of water management (such as irrigation), although it currently considers herbaceous bioenergy crops only. From this perspective, we firmly believe that our enhanced model contributes to the bioenergy crop modelling community and our results are reproducible with the transparent parameter disclosed.

There are still several uncertainties and limitations that need to be addressed in the future. First, the current yield estimations undoubtedly still contain uncertainties. To quantitatively describe such uncertainty, as shown in Fig. S7, we compared our

https://doi.org/10.5194/gmd-2020-179
Preprint. Discussion started: 7 July 2020

simulation with the latest available global bioenergy crop yield map, generated from observations with a random-forest (RF) algorithm (Li et al., 2020). This RF yield map provides a benchmark for evaluating model performance because it is largely constrained by the observed yield ranges, denoting the yields achievable under current technologies (Li et al., 2020). As shown in Fig. S7a and Fig. 7b, small differences between our estimated yield and RF yield exist for switchgrass, whereas larger differences were found for *Miscanthu*, especially in tropical regions. There is a similar case for ORCHIDEE, as shown in Fig. S21 in Li et al. (2020). We also compared the differences in the mean values for *Miscanthus* and Switchgrass because they are not distinguished in LPJmL. As shown in Fig. S7c and Fig. S7d, the differences between our estimations and the RF yield generally were lower than those between LPJml estimations and the RF yield. In summary, our estimations were well within the ranges of those of ORCHIDEE and LPJml. Second, the bioenergy crop yield simulated by H08 did not include constraints due to nutrients, such as nitrogen and phosphorus. Nutrient dynamics are influenced by complex site-specific soil conditions (soil type, temperature, wetness, carbon, etc.), which remain quite challenging to properly represent in global models. This is why similar assumptions and limitations occur in the latest bioenergy potential/yield studies (Li et al., 2018; Yamagata et al., 2018; Wu et al., 2019). Additionally, the effects of CO_2 fertilizer and technological advancements were not considered in the current simulations. Third, our simulation was conducted with historical meteorological drivers. Therefore, variations in yield in future climate scenarios under different representative concentration pathways need to be examined. Fourth, the current irrigation levels were input to represent uniform unconstrained irrigation. Further evaluations need to consider the availability of renewable water sources, and planetary boundaries of land, food, and water (Heck et al., 2018). Finally, as with other models, like MISCANMOD (Clifton-Brown et al., 2004), SWAT (Neitsch et al., 2011), and LPJml (Bondeau et al., 2007), we adopted a crop-uniform water stress formulation. However, an earlier study indicated that the water stress could be crop-specific (Hastings et al., 2009). Additional investigations of the water stress formulation for different bioenergy crops are needed.

4 Conclusion

In this study, we enhanced the ability of the H08 global hydrological model to simulate the yield of a dedicated second-generation herbaceous bioenergy crop. The enhanced H08 model generally performed well in simulating the yield of both *Miscanthus* and switchgrass, with the estimations being well within the range of observations and other model simulations. To the best of our knowledge, this study is the first attempt to successfully enable a global hydrological model with consideration of water management, such as irrigation, to separately simulate the yield of *Miscanthus* and switchgrass. The enhanced model could be a good tool for the future assessment of the bioenergy–water tradeoffs. With this tool, we quantified the effects of irrigation on yield, water consumption, and WUE for both *Miscanthus* and switchgrass in different climate zones. We found that irrigation more than doubled the yield in all areas under rainfed conditions and reduced the WUE by 32%. However, due to the low water consumption in tropical areas, the highest WUE was generally found in tropical climate zones, regardless of whether the crop was irrigated.

Code and data availability. The code of the model used in this study is archived on Zenodo (https://zenodo.org/record/3521407#.XbjZqiXTZMB) under the Creative Commons Attribution 4.0 International License. Technical information about the H08 model and the input dataset are available from the following website: http://h08.nies.go.jp.

Competing interests. The authors declare that they have no conflict of interest.

https://doi.org/10.5194/gmd-2020-179
Preprint. Discussion started: 7 July 2020

Author contribution. Naota Hanasaki designed this study. Zhipin Ai collected the data, developed the model code, and performed the simulations. Zhipin Ai prepared the manuscript, with contributions and comments from Naota Hanasaki, Vera Heck, Tomoko Hasegawa, and Shinichiro Fujimori.

Acknowledgments. This study was funded by the Environment Research and Technology Development Fund (S-14) of the Environmental Restoration and Conservation Agency, Japan.

https://doi.org/10.5194/gmd-2020-179
Preprint. Discussion started: 7 July 2020

References

Anderson, M. C., Norman, J. M., Mecikalski, J. R., Otkin, J. A., and Kustas, W. P. A.: A climatological study of evapotranspiration and moisture stress across the continental United States based on thermal remote sensing: 1. Model formulation, JGR Atmospheres, 112, https://doi:10.1029/2006jd007506, 2007.

Arnold, J. G., Kiniry, J. R., Srinivasan, R., Williams, J. R., Haney, E. B., and Neitsch, S. L. (Eds.): SWAT 2012 Input/Output Documentation, Texas Water Resources Institute, USA, 2013.

Bauer, N., Rose, S. K., Fujimori, S., Van Vuuren, D. P., Weyant, J., Wise, M., Cui, Y., Daioglou, V., Gidden, M. J., Kato, E., Kitous, A., Leblanc, F., Sands, R., Sano, F., Strefler, J., Tsutsui, J., Bibas, R., Fricko, O., Hasegawa, T., Klein, D., Kurosawa, A., Mima, S., Muratori, M.: Global energy sector emission reductions and bioenergy use: overview of the bioenergy demand phase of the EMF-33 model comparison. Clim. Change, 1–16, https://doi.org/10.1007/s10584-018-2226-y, 2018.

Beale C. V., Bint, D. A., Long, S. P.: Leaf photosynthesis in the C4-grass Miscanthus × giganteus, growing in the cool temperate climate of southern England, J. Exp. Bot., 47, 267–273, https://doi.org/10.1093/jxb/47.2.267, 1996.

Beale, C. V., and Long, S. P.: Can perennial C4 grasses attain high efficiencies of radiant energy conversion in cool climates? Plant, Cell Environ., 18, 641–650, https://doi:10.1111/j.1365-3040.1995.tb00565.x., 1995.

Beringer, T. I. M., Lucht, W., and Schaphoff, S.: Bioenergy production potential of global biomass plantations under environmental and agricultural constraints, GCB Bioenergy, 3, 299–312, https://doi:10.1111/j.1757-1707.2010.01088.x, 2001.

Bondeau, A., Smith, P. C., Zaehle, S., Schaphoff, S., Lucht, W., Cramer, W., Gerten, D., Lotze-Campen, H., Müller, C., Reichstein, M., and Smith, B.: Modelling the role of agriculture for the 20th century global terrestrial carbon balance, Glob. Change Biol., 13, 679–706, https://doi:10.1111/j.1365-2486.2006.01305.x, 2007.

Bonsch, M., Humpenöder, F., Popp, A., Bodirsky, B., Dietrich, J. P., Rolinski, S., Biewald, A., Lotze-campen, H., Weindl, I., Gerten, D., and Stevanovic, M.: Trade-offs between land and water requirements for large-scale bioenergy production, GCB Bioenergy, 8(1), 11–724, https://doi:10.1111/gcbb.12226, 2016.

Cheng, Y., Huang, M., Chen, M., Guan, K., Bernacchi, C., Peng, B., and Tan, Z.: Parameterizing perennial bioenergy crops in Version 5 of the Community Land Model based on site-level observations in the Central Midwestern United States, J. Adv. Model. Earth Syst., 12(1), 1–24, https://doi.org/ 10.1029/2019MS001719, 2020.

Clifton-Brown, J. C., Neilson, B., Lewandowski, I., and Jones, M. B.: The modelled productivity of Miscanthus×giganteus (GREEF et DEU) in Ireland, Ind. Crops Prod., 12, 97–109, https://doi:10.1016/S0926-6690(00)00042-X, 2000.

Clifton-Brown, J. C., Stampfl, P. F., and Jones, M. B.: Miscanthus biomass production for energy in Europe and its potential contribution to decreasing fossil fuel carbon emissions, Glob. Change Biol., 10, 509–518, https://doi:10.1111/j.1529-8817.2003.00749.x, 2004.

Giannoulis, K. D., Karyotis, T., Sakellariou-Makrantonaki, M., Bastiaans, L., Struik, P. C., and Danalatos, N. G.: Switchgrass biomass partitioning and growth characteristics under different management practices, NJAS-Wageningen J. Life Sci., 78, 61–67, https://doi.org/10.1016/j.njas.2016.03.011, 2016.

Hanasaki, N., Inuzuka, T., Kanae, S., Oki, T.: An estimation of global virtual. water flow and sources of water withdrawal for major crops and livestock products using a global hydrological model, J. Hydrol., 384, 232–244, https://doi.org/10.1016/j.jhydrol.2009.09.028, 2010.

Hanasaki, N., Kanae, S., Oki, T., Masuda, K., Motoya, K., Shirakawa, N., Shen, Y., Tanaka, K.: An integrated model for the assessment of global water resources – Part 1: Model description and input meteorological forcing, Hydrol. Earth Syst. Sci., 12, 1007–1025, https://doi:10.5194/hess-12-1007-2008, 2008a.

https://doi.org/10.5194/gmd-2020-179
Preprint. Discussion started: 7 July 2020

Hanasaki, N., Kanae, S., Oki, T., Masuda, K., Motoya, K., Shirakawa, N., Shen, Y., and Tanaka, K.: An integrated model for the assessment of global water resources – Part 2: Applications and assessments, Hydrol. Earth Syst. Sci., 12, 1027–1037, https://doi:10.5194/hess-12-1027-2008, 2008b.

Hanasaki, N., Yoshikawa, S., Pokhrel, Y., Kanae, S.: A global hydrological simulation to specify the sources of water used by humans, Hydrol. Earth Syst. Sci., 22, 789–817, https://doi:10.5194/hess-22-789-2018, 2018a.

Hanasaki, N., Yoshikawa, S., Pokhrel, Y., and Kanae, S.: A quantitative investigation of the thresholds for two conventional water scarcity indicators using a state-of-the-art global hydrological model with human activities, Water Resour. Res., 54, 8279–8294, https://doi.org/10.1029/2018WR022931, 2018b.

Hastings, A., Clifton-Brown, J., Wattenbach, M., Mitchell, C. P., and Smith, P.: The development of MISCANFOR, a new *Miscanthus* crop growth model: towards more robust yield predictions under different climatic and soil conditions, GCB Bioenergy, 1, 154–170, https://doi:10.1111/j.1757-1707.2009.01007.x, 2009.

Heaton, E. A., Boersma, N., Caveny, J. D., Voigt, T. B., and Dohleman, F. G.: Miscanthus for biofuel production,available at: https://farm-energy.extension.org/miscanthus-miscanthus-x-giganteus-for-biofuel-production/, 2019.

Heaton, E. A., Dohleman, F. G., and Long, S. P.: Meeting US biofuel goals with less land: the potential of Miscanthus, Glob. Change Biol., 14, 2000–2014, https://doi:10.1111/j.1365-2486.2008.01662.x, 2008.

Heck, V., Gerten, D., Lucht, W., and Boysen, L. R.: Is extensive terrestrial carbon dioxide removal a 'green' form of geoengineering? A global modelling study, Glob. Planet. Change, 137, 123–130, https://doi:10.1016/j.gloplacha.2015.12.008, 2016.

Heck, V., Gerten, D., Lucht, W., and Popp, A.: Biomass-based negative emissions difficult to reconcile with planetary boundaries, Nat. Clim. Change, 8, 151–155, https://doi:10.1038/s41558-017-0064-y, 2018.

Hejazi, M. I., Voisin, N., Liu, L., Bramer, L. M., Fortin, D. C., Hathaway, J. E., Huang, M., Kyle, P., Leung, L. R., Li, H. Y., Liu, Y., Patel, P., Pulsipher, P. L., Rice, J. S., Tesfa, T. K., Vernon, C. R., Zhou, Y.: 21st century United States emissions mitigation could increase water stress more than the climate change it is mitigating, Proc. Natl. Acad. Sci. USA, 112(34), 10635–10640, https://doi.org/10.1073/pnas.1421675112, 2015.

Iizumi, T., Takikawa, H., Hirabayashi, Y., Hanasaki, N., and Nishimori, M.: Contributions of different bias-correction methods and reference meteorological forcing data sets to uncertainty in projected temperature and precipitation extremes. JGR Atmospheres, 122, 7800-7819, https://doi.org/10.1002/2017JD026613, 2017.

Kang, S., Nair, S. S., Kline, K. L., Nichols, J. A., Wang, D., Post, W. M., Brandt, C. C., Wullschleger, S. D., Singh, N., Wei, Y.: Global simulation of bioenergy crop productivity: analytical framework and case study for switchgrass, GCB Bioenergy, 6, 14–25, https://doi:10.1111/gcbb.12047, 2014.

Lewandowski, I., Scurlock, J. M., Lindvall, E., and Christou, M.: The development and current status of perennial rhizomatous grasses as energy crops in the US and Europe, Biomass Bioenerg., 25, 335–361, https://doi:10.1016/S0961-9534(03)00030-8, 2003.

Li, W., Ciais, P., Makowski, D., and Peng, S.: A global yield dataset for major lignocellulosic bioenergy crops based on field measurements, Sci. Data, 5, 180169, https://doi:10.1038/sdata.2018.169, 2018a.

Li, W., Yue, C., Ciais, P., Chang, J., Goll, D., Zhu, D., Peng, S., and Jornet-Puig, A.: ORCHIDEE-MICT-BIOENERGY: an attempt to represent the production of lignocellulosic crops for bioenergy in a global vegetation model, Geosci. Model Dev., 11, 2249–2272, https://doi.org/10.5194/gmd-11-2249-2018, 2018b.

Li, W., Ciais, P., Stehfest, E., van Vuuren, D., Popp, A., Arneth, A., Di Fulvio, F., Doelman, J., Humpenöder, F., Harper, A. B., Park, T., Makowski, D., Havlik, P., Obersteiner, M., Wang, J., Krause, A., and Liu, W.: Mapping the yields of lignocellulosic bioenergy crops from observations at the global scale, Earth Syst. Sci. Data, 12, 789–804, https://doi.org/10.5194/essd-12-789-2020, 2020.

https://doi.org/10.5194/gmd-2020-179
Preprint. Discussion started: 7 July 2020

Madakadze, I. C., Stewart, K., Peterson, P. R., Coulman, B. E., Samson, R., and Smith, D. L.: Light interception, use-efficiency and energy yield of switchgrass (Panicum virgatum L.) grown in a short season area, Biomass Bioenerg., 15, 475–482, https://doi.org/10.1016/S0961-9534(98)00060-9, 1998.

Mclsaac, G. F., David, M. B., and Mitchell, C. A.: Miscanthus and switchgrass production in central Illinois: impacts on hydrology and inorganic nitrogen leaching, J. Environ. Qual., 39, 1790–1799, https://doi:10.2134/jeq2009.0497, 2010.

Mo, X., Liu, S., Lin, Z., Xu, Y., Xiang, Y., and McVicar, T. R.: Prediction of crop yield, water consumption and water use efficiency with a SVAT-crop growth model using remotely sensed data on the North China Plain, Ecol. Modell., 183, 301–322, https://doi:10.1016/j.ecolmodel.2004.07.032, 2005.

Monteith, J. L., Moss, C. J., Cooke George, W., Pirie Norman, W., and Bell George Douglas, H.: Climate and the efficiency of crop production in Britain. Philosophical Transactions of the Royal Society of London, B, Biol. Sci., 281, 277–294. https://doi:10.1098/rstb.1977.0140, 1977.

Nichols, J., Kang, S., Post, W., Wang, D., Bandaru, V., Manowitz, D., and Zhang, X., Izaurralde, R.: HPC-EPIC for high resolution simulations of environmental and sustainability assessment, Comput. Electron. Agric., 79, 112–115, https://doi:10.1016/j.compag.2011.08.012, 2011.

Neitsch, S. L., Arnold, J. G., Kiniry, J. R., and Williams, J. R. Soil and water assessment tool theoretical documentation version 2009. Texas Water Resources Institute, Texas, US, 2011.

Ojeda, J. J., Volenec, J. J., Brouder, S. M., Caviglia, O. P., and Agnusdei, M. G.: Evaluation of Agricultural Production Systems Simulator as yield predictor of *Panicum virgatum* and *Miscanthus x giganteus* in several US environments, GCB Bioenergy, 9, 796–816, https://doi:10.1111/gcbb.12384, 2017.

Oweis, T., Zhang, H., and Pala, M.: Water use efficiency of rainfed and irrigated bread wheat in a Mediterranean environment, Agron. J., 92, 231–238, https://doi:10.2134/agronj2000.922231x, 2000.

Rose, S. K., Kriegler, E., Bibas, R., Calvin, K., Popp, A., van Vuuren, D. P., and Weyant, J.: Bioenergy in energy transformation and climate management, Clim. Change, 123, 477–493, https://doi:10.1007/s10584-013-0965-3, 2013.

Searle, S. Y., and Malins, C. J.: Will energy crop yields meet expectations?, Biomass Bioenerg., 65, 3–12, https://doi:10.1016/j.biombioe.2014.01.001, 2014.

Smith, P., Davis, S. J., Creutzig, F., Fuss, S., Minx, J., Gabrielle, B., Kato, E., Jackson, R. B., Cowie, A., Kriegler, E., van Vuuren, D. P., Rogelj, J., Ciais, P., Milne, J., Canadell, J. G., McCollum, D., Peters, G., Andrew, R., Krey, Volker., Shrestha, G., Friedlingstein, P., Gasser, T., Grübler, A., Heidug, W. K., Jonas, M., Jones, C. D., Kraxner, F., Littleton, E., Lowe, J., Moreira, J. R., Nakicenovic, N., Obersteiner, M., Patwardhan, A., Rogner, M., Rubin, E., Sharifi, A., Torvanger, A., Yamagata, Y., Edmonds, J., and Yongsung, C.: Biophysical and economic limits to negative CO2 emissions, Nat. Clim. Change, 6, 42–50, https://doi:10.1038/nclimate2870, 2015.

Trybula, E. M., Cibin, R., Burks, J. L., Chaubey, I., Brouder, S. M., and Volenec, J. J.: Perennial rhizomatous grasses as bioenergy feedstock in SWAT: parameter development and model improvement, GCB Bioenergy, 7, 1185–1202, https://doi:10.1111/gcbb.12210, 2015.

VanLoocke, A., Twine, T. E., Zeri, M., and Bernacchi, C. J.: A regional comparison of water use efficiency for *Miscanthus*, switchgrass and maize, Agric. Forest Meteorol., 164, 82–95, http://dx.doi.org/10.1016/j.agrformet.2012.05.016, 2012.

van der Werf, H. M. G., Meijer, W. J. M., Mathijssen, E. W. J. M., and Darwinkel, A.: Potential dry matter production of Miscanthus sinensis in the Netherlands, Ind. Crops Prod., 1, 203–210, https://doi:10.1016/0926-6690(92)90020-V, 1992.

Weedon, G. P., Balsamo, G., Bellouin, N., Gomes, S., Best, M. J., and Viterbo, P.: The WFDEI meteorological forcing data set: WATCH Forcing Data methodology applied to ERA-Interim reanalysis data, Water Resour. Res., 50(9), 7505–7514, https://doi.org/10.1002/2014WR015638, 2014.

https://doi.org/10.5194/gmd-2020-179
Preprint. Discussion started: 7 July 2020

Yamagata, Y., Hanasaki, N., Ito, A., Kinoshita, T., Murakami, D., and Zhou, Q.: Estimating water–food–ecosystem trade-offs for the global negative emission scenario (IPCC-RCP2.6), Sustainability Sci., 13(2), 301–313, https://doi:10.1007/s11625-017-0522-5, 2018.

Yao, Y., Liang, S., Qin, Q., and Wang, K.: Monitoring drought over the conterminous United States using MODIS and NCEP Reanalysis-2 data, J. Appl. Meteorol. Climatol., 49(8), 1665–1680. https://doi:10.1175/2010jamc2328.1, 2010.

Wu, W., Hasegawa, T., Ohashi, H., Hanasaki, N., Liu, J., Matsui, T., Fujimori, S., and Takahashi, K.: Global advanced bioenergy potential under environmental protection policies and societal transformation measures, GCB Bioenergy, 11(9), 1041–1055, https://doi.org/10.1111/gcbb.12614, 2019.

https://doi.org/10.5194/gmd-2020-179
Preprint. Discussion started: 7 July 2020

Geoscientific Model Development Discussions
Open Access
EGU

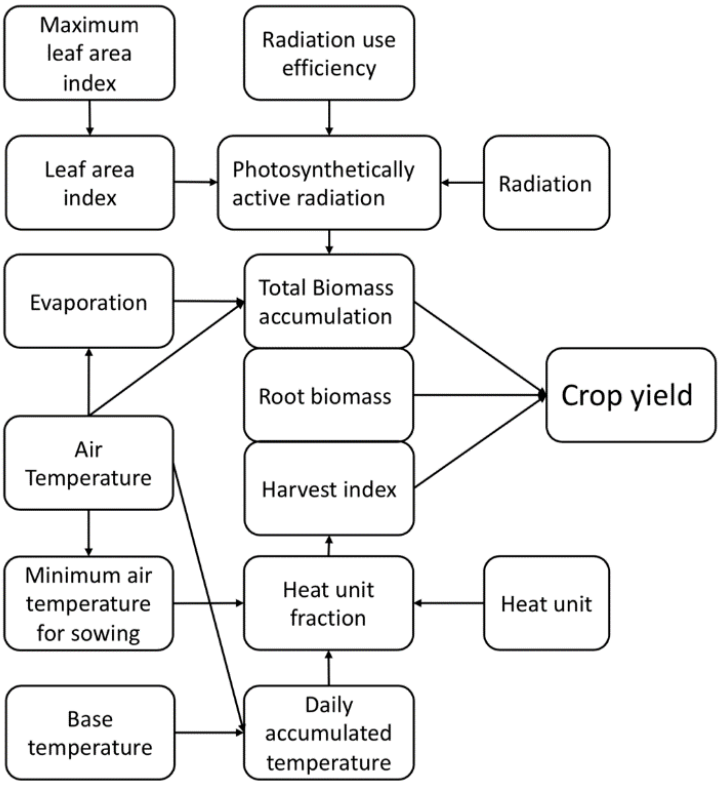

Fig. 1 Schematic diagram showing the basic biophysical process of the crop module in the H08 model.

https://doi.org/10.5194/gmd-2020-179
Preprint. Discussion started: 7 July 2020

Geoscientific Model Development
Discussions
Open Access
EGU

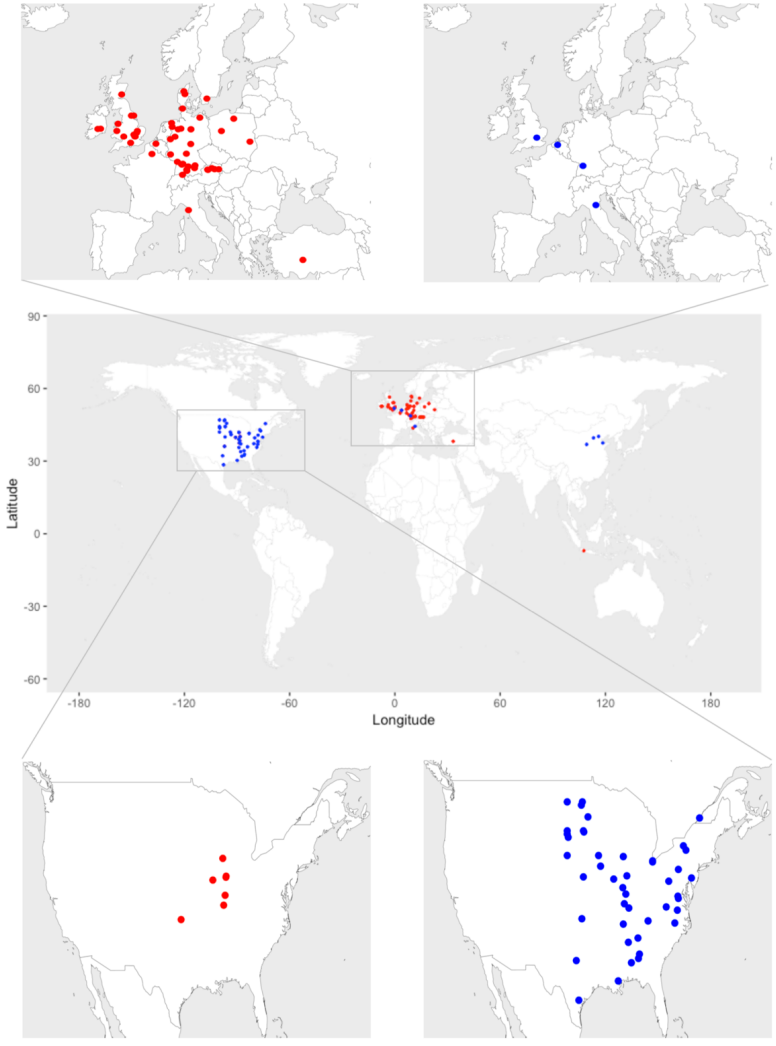

Fig. 2 Map showing the locations of the *Miscanthus* (red dots) and switchgrass (blue dots) sites under rainfed condition.

https://doi.org/10.5194/gmd-2020-179
Preprint. Discussion started: 7 July 2020

Geoscientific Model Development
Discussions
Open Access
EGU

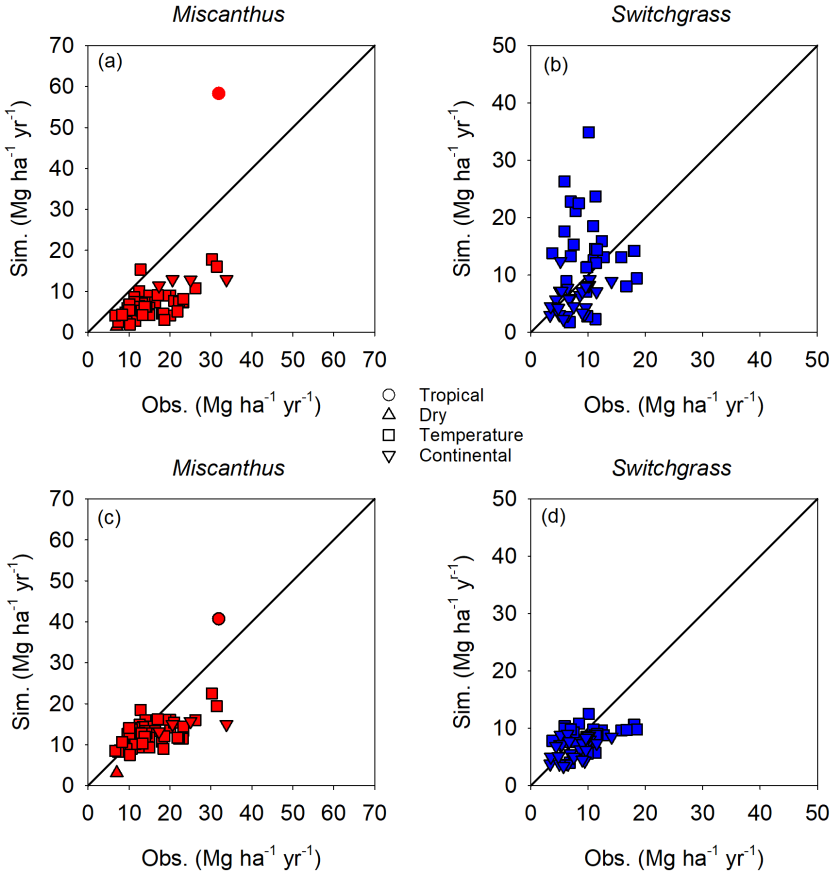

Fig. 3 Overall comparison of the simulated (Sim.) and observed (Obs.) yields for *Miscanthus* and switchgrass, respectively. The simulated yields in (a) and (b) are from the original H08 model, whereas those in (c) and (d) are from the enhanced H08 model. The black line is the 1:1 line.

https://doi.org/10.5194/gmd-2020-179
Preprint. Discussion started: 7 July 2020

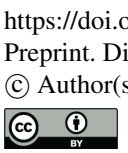

Geoscientific Model Development Discussions

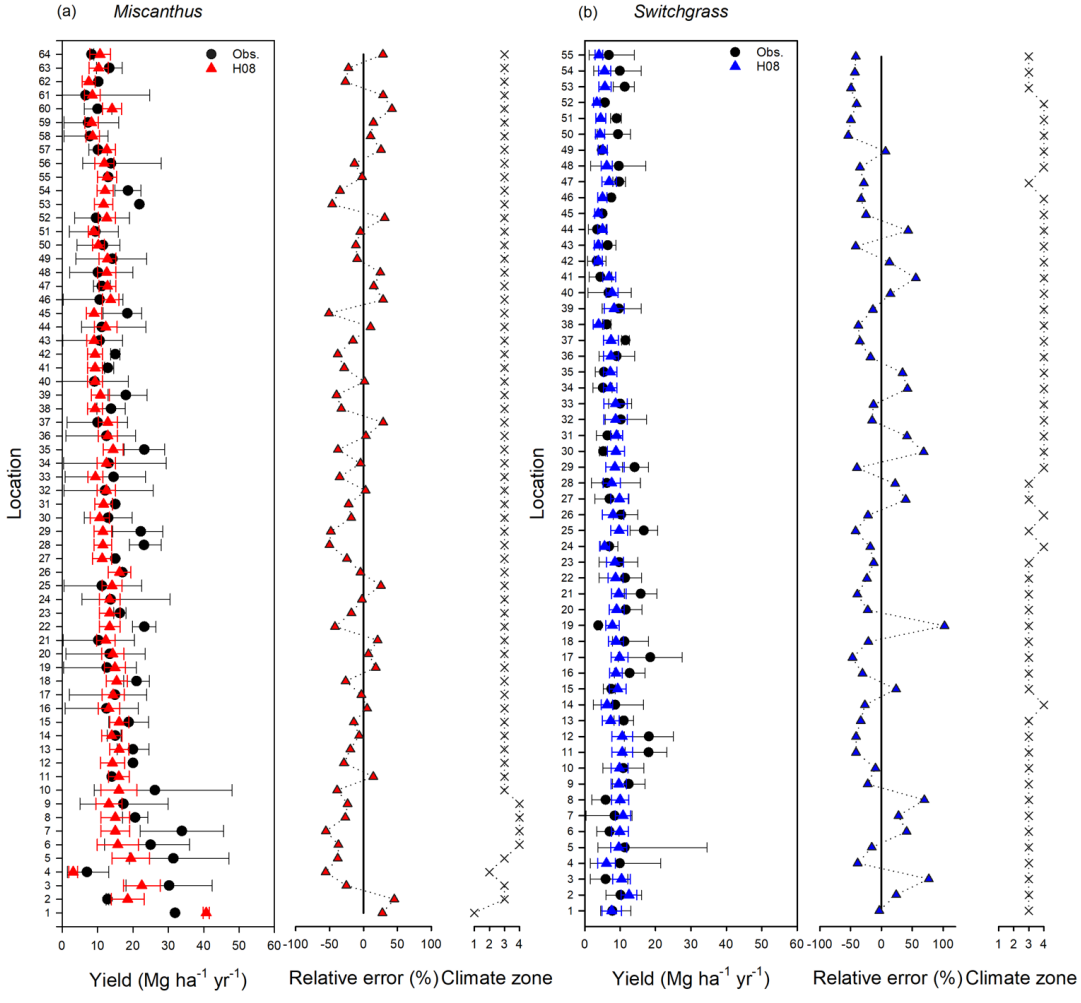

Fig. 4 Site-specific performance (presented with latitude increasing from the bottom of the vertical axis) and relative error of the simulated yield obtained using the enhanced H08 model compared with the observed yields for *Miscanthus* and switchgrass. The longitude and latitude of each location for *Miscanthus* and switchgrass are given in Tables S1 and S2, respectively. The thin "x" indicates the site's climate, where 1, 2, 3, and 4 refer to the tropical, dry, temperature, and continental climate zone, respectively. Obs. means the observed mean yield. The error bar in black color represents the range of the observed minimum and maximum yield, respectively. The error bar in red or blue color represents the standard deviation of the simulated yield from 1979 to 2016.

https://doi.org/10.5194/gmd-2020-179
Preprint. Discussion started: 7 July 2020

Geoscientific Model Development Discussions
Open Access
EGU

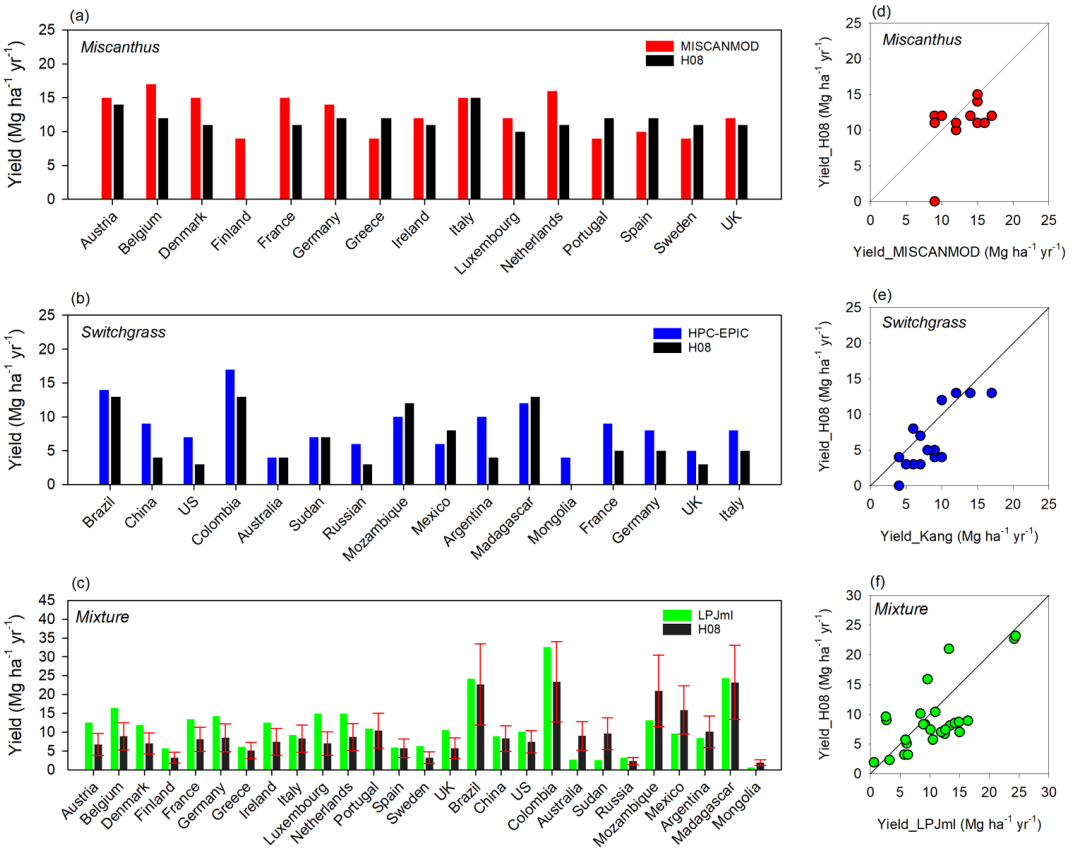

Fig. 5 An independent country-specific comparison of the simulated yield by the enhanced H08 model with those of three other models (MISCANMOD, HPC-EPIC, and LPJmL) for *Miscanthus* (a, d), switchgrass (b, e), and their combination (c, f), respectively. The H08 in (c, f) indicates the average yield of *Miscanthus* and switchgrass, and the upper and lower error bars in (c) represent the yields for *Miscanthus* and switchgrass, respectively.

https://doi.org/10.5194/gmd-2020-179
Preprint. Discussion started: 7 July 2020

Geoscientific Model Development
Discussions
Open Access
EGU

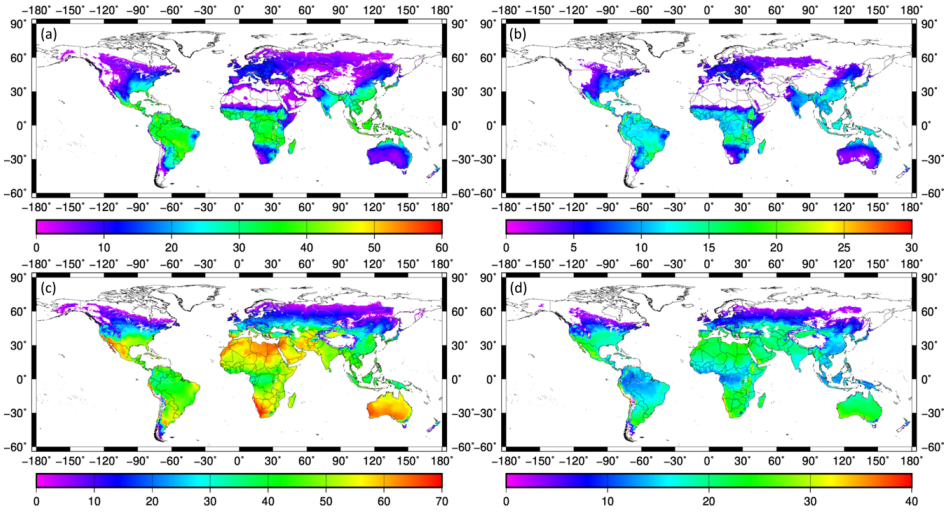

Fig. 6 Spatial distributions of the simulated yields (exceeds 2 Mg ha^{-1} yr^{-1}) for *Miscanthus* (a, c) and switchgrass (b, d) under rainfed (a, b) and irrigated (c, d) conditions, respectively. The unit for the legend is Mg ha^{-1} yr^{-1}.

https://doi.org/10.5194/gmd-2020-179
Preprint. Discussion started: 7 July 2020

Geoscientific Model Development Discussions
Open Access
EGU

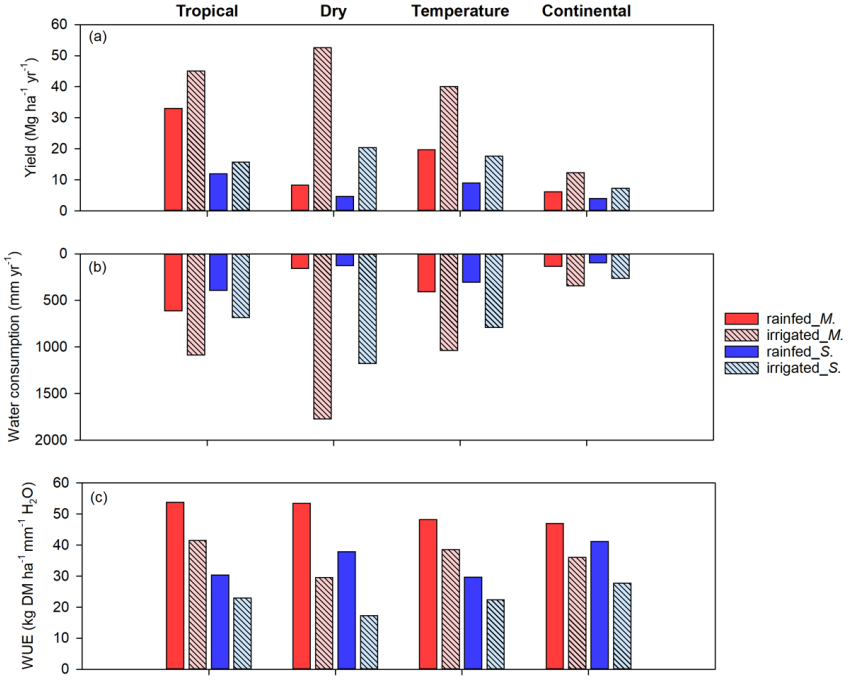

Fig. 7 Variations in the average yield (a), crop water consumption (b), and water use efficiency (WUE) (c) for *Miscanthus* and switchgrass under rainfed and irrigated conditions in four different Köppen climate zones (tropical, dry, temperate, and continental climates) based on meteorology data collected from 1979 to 2016. The abbreviations *M.* and *S.* in the legend denote *Miscanthus* and switchgrass, respectively.

https://doi.org/10.5194/gmd-2020-179
Preprint. Discussion started: 7 July 2020

Geoscientific Model Development Discussions

Table 1. Parameters set in the enhanced H08 model.

85

Bioenergy crop	Parameter	Value	Source
Miscanthus	Hun	1,830	Trybula et al., (2015)
	be	38	Calibrated
	To	25	Trybula et al., (2015); Hastings et al., (2009)
	Tb	8	Calibrated
	blai	11	Calibrated
	dlai	1.1	Trybula et al., (2015)
	dpl1	10.1	Trybula et al., (2015)
	dpl2	45.85	Trybula et al., (2015)
	rdmx	3	Trybula et al., (2015)
	Hunmax	11.5	Calibrated
	TSAW	8.0	Calibrated
Switchgrass	Hun	1,400	Trybula et al., (2015)
	be	22	Calibrated
	To	25	Trybula et al., (2015)
	Tb	10	Calibrated
	blai	8	Calibrated
	dlai	1	Trybula et al., (2015)
	dpl1	10.1	Trybula et al., (2015)
	dpl2	40.85	Trybula et al., (2015)
	rdmx	3	Trybula et al., (2015)
	Hunmax	15.5	Calibrated
	TSAW	8.0	Calibrated

https://doi.org/10.5194/gmd-2020-179
Preprint. Discussion started: 7 July 2020

Geoscientific Model Development Discussions
Open Access
EGU

Table 2. Parameter ranges and steps for calibration simulations.

Bioenergy crop	Parameter	Range	Step	Unit	Reference
Miscanthus	be	(30, 40)	2	g MJ^{-1} × 10	Clifton-Brown et al., (2000); van der Werf et al., (1992); Beale and Long, (1995); Heaton et al., (2008); Trybula et al., (2015)
	blai	(9, 11)	1	m^2 m^{-2}	Heaton et al., (2008); Trybula et al., (2015)
	Tb	(7, 9)	1	℃	Beale et al., (1996); Trybula et al., (2015)
	Hunmax	(11.5, 16.5)	1	℃	H08 Endogenous variable
	TSAW	(8, 10)	1	℃	H08 Endogenous variable
Switchgrass	be	(12, 22)	2	g MJ^{-1} × 10	Heaton et al., (2008); Madakadze et al., (1998); Trybula et al., (2015)
	blai	(6, 8)	1	m^2 m^{-2}	Trybula et al., (2015); Giannoulis et al., (2016); Madakadze et al., (1998); Heaton et al., (2008)
	Tb	(8, 10)	1	℃	Trybula et al., (2015)
	Hunmax	(11.5, 16.5)	1	℃	H08 Endogenous variable
	TSAW	(8, 10)	1	℃	H08 Endogenous variable